

Design of the Hydraulically-Actuated, Torque-Controlled Quadruped Robot HyQ2Max

Claudio Semini, *Member, IEEE*, Victor Barasuol, Jake Goldsmith, Marco Frigerio, Michele Focchi, Yifu Gao, *Student Member, IEEE*, and Darwin G. Caldwell *Member, IEEE*

Abstract—This paper presents the design of the hydraulically actuated quadruped robot *HyQ2Max*. *HyQ2Max* is an evolution of the 80kg agile and versatile robot *HyQ*. Compared to *HyQ*, the new robot needs to be more rugged, more powerful and extend the existing locomotion skills with self-righting capability. Since the robot's actuation system has an impact on many aspects of the overall design/specifications of the robot (e.g. payload, speed, torque, overall mass, compactness), this paper will pay special attention to the selection and sizing of the joint actuators. To obtain meaningful joint requirements for the new machine, we simulated 7 characteristic motions that cover a wide range of required behaviors of an agile rough terrain robot, including trotting on rough terrain, stair climbing, push recovery, self-righting, etc. We will describe how to use the obtained joint requirements for the selection of the hydraulic actuator types, four-bar linkage parameters and valve size. Poorly sized actuators may lead to limited robot capabilities or higher cost, weight, energy consumption and cooling requirements. The main contributions of this paper are (1) a novel design of an agile quadruped robot capable of performing trotting/crawling over flat/uneven terrain, balancing and self-righting; (2) a detailed method to find suitable hydraulic cylinder/valve properties and linkage parameters with a specific focus on optimizing the actuator areas; and (3) to the best knowledge of the authors, the most complete review of hydraulic quadruped robots.

I. INTRODUCTION

LEGGED robots have the potential to become a new generation of rough terrain vehicles that are capable of autonomous, semi-autonomous or remote-controlled operations in challenging terrains where wheeled and tracked vehicles reach their limits. In the future, legged vehicles will assist or replace humans in dangerous and dirty tasks. Quadruped robots are expected to operate in highly dynamic, unstructured outdoor areas where they will navigate inside challenging environments, such as collapsed buildings, disaster (natural and man-made) sites, forests, mountain farms and construction sites. Their tasks will range from providing sensor streams to the remote operator (e.g. cameras, LIDAR, infrared, radiation levels) to carrying heavy payloads such as tools or building materials. Different applications will impose different requirements on the machine. A transport robot over rough terrain for example needs high-torque actuators to carry substantial payloads. An agile inspection robot that has to enter a disaster area to give rescue workers and firemen a map with

danger zones (e.g. infrared images inside a burning building) needs to be fast and agile with small payload requirements. A military specified robot such as Boston Dynamics' LS3 may require a quiet or stealth mode. The robot's intended application will therefore strongly influence the requirements on mechanical design, actuation, acoustic signature, noise levels, fuel efficiency, etc.

Today's robot designers, however, rarely follow a systematic approach based on application specifications to correctly size body structures, linkage mechanisms and actuators. However, the nature of the actuation, which affects and possibly controls features such as: payload, speed, torque, overall mass, compactness, can be seen as a key driver in determining many of the critical design decisions in the construction of the robot. There are three main design parameters that need to be determined for each actuated joint: range of motion, maximum torque output profile and maximum velocity output profile. These three parameters are often estimated based on kinematics/dynamics data of humans or animals (e.g., [1], [2], [3]) or based on simulations of simplified robot models for 1-2 motions only (e.g., [4], [5], [6], [7], [8]). However, biological data and oversimplified simulations will not cover appropriately the full range of desired motions and will lead to suboptimal designs of legged robots.

A second, more ad hoc, approach is to first build the robot with available actuators that fit inside the robot limbs and then test the machine to identify its performance limits (e.g. [9]). While this method is fine for research platforms that push the state of the art, it is not very systematic and does not permit systems design with a specific performance and application goal. Poorly sized actuators have a negative impact on the entire robot: While undersized actuators will limit the robot's capabilities, oversized actuators may lead to higher costs, weight, size, energy consumption and cooling requirements (see Section V).

There are two main reasons for this lack of more systematic design methods in legged robots: First, the problem as a whole is extremely complex since it includes design parameters that cover robot morphology, kinematics, actuators, as well as gait types and gait parameters. Second, since real application scenarios for quadrupeds are rare and ill defined, it is often a challenge for the designer to obtain a suitable list of task requirements¹.

¹Exceptions are for example the RoboCup Rescue Challenge and the recent DARPA Robotics Challenge in 2015 that offered a clear scenario with several detailed tasks descriptions. However, whether these tasks can sufficiently well represent a real disaster scenario is unclear.

Manuscript received November 2, 2015; revised April 23, 2016; accepted August 25, 2016. Date of publication XXX, 2016.

All authors are with the Department of Advanced Robotics, Istituto Italiano di Tecnologia (IIT), 16163 Genova, Italy. e-mail: firstname.lastname@iit.it, phone: +39 01071781912

IIT's Dynamic Legged Systems lab² has developed a number of torque-controlled quadruped robots since 2007, including HyQ [4], MiniHyQ [10] and most recently, HyQ2Max, see Fig. 1. The long-term goal of the project is to develop the hardware, software and algorithms that will lead to quadruped vehicles that can be tailored to a given application.

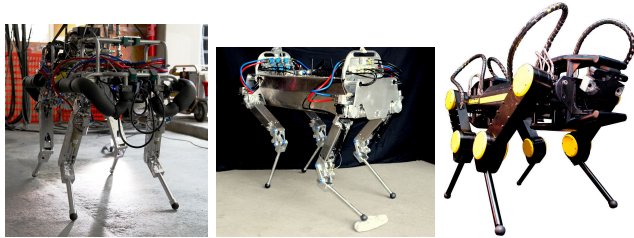


Fig. 1. Pictures of IIT's hydraulic quadruped robot HyQ, MiniHyQ and HyQ2Max. Left: The HyQ robot [4] at an outdoor test track in 2013. Center: MiniHyQ [10] inside the lab in 2015. Right: HyQ2Max robot with white background in 2015.

The hydraulic quadruped robot HyQ [4] is our flagship platform. Since 2010, it demonstrated a wide repertoire of versatile motions including stair climbing [11], walking/trotting over obstacles [12], flying trotting [13] and jumping [14]. Section III-B provides a detailed description of the robot. The experiences with HyQ have helped to create a list of requirements that an upgraded quadruped will need to have. Among the most critical of these issues observed in quadrupeds such as HyQ is robustness (on all levels), but particularly: (a) rugged design that can cope with falls; (b) self-righting capability; (c) ability to squat and lie down on belly; (d) match or exceed HyQ's performance; (e) not heavier than HyQ (with offboard power supply); (f) ability to be retrofitted with an onboard power supply.

This paper describes the most important aspects of the design of HyQ2Max³, that is heavily based on the morphology, torque control and hydraulic actuation technology of HyQ. After the presentation of the prior art (Section II) and robot requirements (III), we will show how simulations of characteristic motions help to obtain meaningful joint position, velocity and torque profiles (Section IV). We will then focus on a method to correctly map these profiles into actuator and mechanism requirements and sizes (Section V). Section VI presents the design of the whole robot, lists its specifications and shows experimental results of the new robot demonstrating self-righting and trotting. A discussion and conclusion end the paper (Section VII and VIII).

The main contributions of this paper are (1) a novel design of an agile quadruped robot capable of performing trotting/crawling over flat/uneven terrain, balancing and self-righting; (2) a detailed method to find suitable hydraulic cylinder/valve properties and linkage parameters with a specific focus on optimizing the actuator areas; and (3) to the best knowledge of the authors, the most complete review of hydraulic quadruped robots.

²URL: <http://www.iit.it/en/advr-labs/dynamic-legged-systems.html>

³We have presented a short overview of HyQ2Max at the 2015 Scandinavian International Conference on Fluid Power [15].

TABLE I
 AN OVERVIEW OF HYDRAULICALLY ACTUATED QUADRUPED ROBOTS

Name	Nationality	Year*	Mass [kg] off/on-board power	DoF per leg
GE truck [16]	USA	1968	NA / 1400	3
Raibert's Quadruped [17]	USA	1986	31.2 / NA	3
TITAN XI [18]	Japan	2007	NA / 7000	3
BigDog [19] **	USA	2008	NA / 109	4
LS3/AlphaDog **	USA	2012	NA / NA	3
Cheetah **	USA	2012	33 / NA	2
Wildcat **	USA	2013	NA / NA	3
Spot **	USA	2015	NA / 72.5	3
SCalf [20]	China	2012	65 / <120	3
Baby Elephant [21]	China	2014	130 / 160	3
BIT quadruped robot [22]	China	2013	NA / 120	4
NUDT quadruped robot [23]	China	2013	NA / NA	4
JINPOONG [24]	Korea	2013	NA / 120	4
RLA-1 [25]	Japan	2014	NA / NA	3
HyQ [4]	Italy	2011	80 / NA	3
MiniHyQ [10]	Italy	2015	24 / NA	3
HyQ2Max (this paper)	Italy	2015	80 / NA	3

* year of citation or first online video

** www.bostondynamics.com

II. STATE OF THE ART

This section is divided into two parts: First, we will present the state of the art in hydraulic quadruped robots. Second, we will give a short overview of the design approaches used to choose and size the actuators of a number of legged robots.

A. Hydraulic Quadruped Robots

Since the main contribution of this paper is the description of the novel design of an agile and versatile quadruped robot with hydraulic actuation, we will provide a survey of the state of the art in hydraulic quadruped robots. To the best knowledge of the authors, this survey is the most complete review of hydraulic quadruped robots. An overview of these robots is shown in Table I. The *Mass* column lists the robot mass with either the power pack offboard or onboard. The abbreviation *NA* is used if no information is available.

The earliest hydraulically powered quadruped robot was the General Electric walking truck, developed in the 1960's by Mosher and Liston [16]. The GE truck was 3.3m tall and weighed 1400kg. The onboard operator was controlling each of the four legs with one of his own limbs through handles and pedals. The robot demonstrated slow walking on flat ground, pushing of obstacles and walking over piles of wooden blocks.

Titan XI is a large size hydraulically actuated quadruped robot developed at the Hirose Lab of the Tokyo Institute of Technology, Japan. The 7000kg robot is designed for construction work on slopes [18]. The robot was able to perform statically stable walking on flat ground and slopes.

Six out of the 17 robots in the list are developed by Marc Raibert and his teams at the CMU Leg lab, MIT Leg lab

(Raibert's Quadruped [17]) and later at Boston Dynamics Inc. (BigDog [19], LS3, Cheetah, WildCat, Spot). Unfortunately, Boston Dynamics has not published any details about the robot designs (e.g. joint range of motion, torque profiles, hydraulic system, power plots, etc.).

Another group of hydraulic quadrupeds were developed in China since 2011 in a well-funded effort to create a Chinese version of BigDog. Several Chinese universities developed their own robot (e.g. SCalf [20], Baby Elephant [21], Beijing Institute of Technology (BIT) quadruped [22], National University of Defense Technology (NUDT) quadruped [23]). Korea has developed a few hydraulic quadruped robot designs within the *Jinpoong project*. Most of these projects are funded by military grants and thus there are not many publications about the robot designs available. Hyon et al. have developed a hydraulic quadruped robot called RLA-1 [25].

As mentioned in the introduction, the Dynamic Legged System lab of the Istituto Italiano di Tecnologia (IIT) has developed 3 hydraulic quadruped robots (HyQ, MiniHyQ, HyQ2Max) since 2007 in a still ongoing effort to develop an agile, rough terrain vehicle for outdoor application. The design of the newest robot, HyQ2Max, is presented in this paper.

B. Robot Design Approaches for Actuator Selection

Another contribution of this paper is the detailed description of how to find suitable four-bar linkage parameters, joint range of motion, actuator piston/annulus/vane areas and valve size. Thus, this section will first survey the prior art in defining suitable kinematics and joint performance requirements of legged robots⁴. The prior art can roughly be divided into 6 categories (with some overlaps). Kinematics and/or joint requirements are usually based on (a) biomechanical studies of humans or animals (e.g. Hyon et al. [2], Seok et al. [3]); (b) simulations of one or several motions with a simplified model (e.g. De et al. [26], Semini et al. [14]); (c) rigid body dynamics simulations of the complete 3D model performing one or several motions (e.g. Kaneko et al. [27], Dallali et al [28] and Rong et al. [29]); (d) optimization of robot morphology and joint requirements (e.g. Geijtenbeek et al. [30], Digumarti et al. [31]); (e) experience with earlier robot prototypes (e.g. De et al. [26]); (f) availability of previously developed, compact, high-performance actuator units (e.g. Ito et al. [9]).

Next, we will present a brief classification of the prior art related to the mapping of joint requirements into actuator space. The most related works can be divided into two groups: (a) electric motors and gears are selected based on continuous and intermittent maximum torque requirements. Each joint is actuated either by a custom-sized motor/gear unit or more commonly, by the best matching unit selected from 2-3 standard sizes, e.g. [28]; (b) linear hydraulic/electric actuators, which actuate a rotational joint, need to be combined with an attachment mechanism (such as a simple hinge joint, four-bar linkage, crossed four-bar linkage) whose geometry and parameters have a direct impact on the mapping, e.g. [4], [32], [33].

⁴Note that the literature on legged robot design is vast. We tried to include a selection of the most representative works.

III. HYQ2MAX PERFORMANCE REQUIREMENTS AND KINEMATICS

This section describes the application requirements for the new robot and analyzes the specifications, skills and limitations of HyQ, the robot that serves as the base for the new design. The section will then list the various motion skills that are needed to meet the application requirements. These skills will later be used to perform simulations (cf. Section IV) to finally obtain actuator specifications (cf. Section V).

Finally, this section discusses the differences in robot kinematics between HyQ and HyQ2Max that will allow the new robot to perform some of the most important required motions.

A. Target Application Requirements

As mentioned in the introduction, legged service robots for rugged outdoor environments are still far from a widespread commercial use. Only a few industries seriously think of specific applications where these robots can be deployed, e.g. nuclear disaster relief (e.g. Toshiba's quadruped robot), inspection (e.g. StarlETH robot in ARGOS challenge [34]), military (e.g. BostonDynamics' robots) and entertainment (e.g. Disney theme parks). On one hand, this is due to the fact that the related technologies (e.g. controllers and hardware) are not sufficiently reliable and advanced yet. On the other hand, cheaper and less complicated solutions with wheels and tracks can often match (and outperform) the current performance of the legged robot prototypes. Without the input of the industry to provide clear use cases of future legged service robots, it is difficult for the robot designers to obtain detailed application requirements based on which they can correctly design their robots.

HyQ2Max has to serve as research prototype to further advance the state of the art in robust robot hardware and controllers, without a specific application in mind. The final goal is to create a demonstrator platform that can prove superior mobility and agility on rough terrain compared to traditional vehicles.

We defined the following list of requirements for the new robot, based on the above goal and our experience with HyQ (see Section III-B):

- 1) *rugged design that can cope with falls*: The mechanical structure needs to be sufficiently strong and rugged to allow the robot to fall without damage.
- 2) *self-righting capability*: The robot needs to be able to get up on its own after falling. This should be a fundamental skill of any legged robot, since all of them will fall at some point, during the execution of a real-world task.
- 3) *ability to squat and lie down on belly*: This allows the robot to save energy during waiting periods and makes its transport easier.
- 4) *match or exceed HyQ's performance*: This allows the robot to perform more agile motions than HyQ, which will push the state of art in quadruped motion planning and control.
- 5) *not heavier than HyQ*: The existing weight of HyQ (80kg) turned out to be a good compromise between ease of operation/transport (3-4 people can easily lift it)

TABLE II
SYSTEM OVERVIEW OF THE HYQ ROBOT

dimensions	1.0m x 0.5m x 0.98m (LxWxH)
link lengths & weights	hip (HAA-HFE): 0.08m, 2.9kg upper leg (HFE-KFE): 0.35m, 2.6kg lower leg (KFE-foot): 0.35m, 0.8kg
weight	80kg
active DOF	12
HAA actuators	double-vane rotary hydraulic actuators
HFE/KFE actuators	asymmetric hyd. cylinders with hinge joint
joint motion range	90° (HAA), 120° (HFE, KFE)
max. torque [HAA]	120Nm (peak torque at 20MPa)
max. torque [HFE/KFE]	181Nm (peak torque at 20MPa)
position sensors	position 80000cpr in all joints
torque sensors	custom torque (HAA), loadcell (HFE, KFE)
onboard computer	Pentium i5 with real-time Linux
controller rate	1kHz

and size that allows mounting of tools and carrying a useful payload in the future (see next point).

- 6) *ability to be retrofitted with an onboard power supply:* The legs should be strong enough to carry an onboard power supply in the future (maximum 40kg extra weight including payload). This way, only the torso needs to be updated.

B. HyQ Robot Overview, Skill and Limitations

The above-mentioned requirements are based on our experience with HyQ, Fig. 1 (left). This section will thus first provide a short overview of HyQ's specifications and skills, to then assess the limitations of the machine that will lead to a better understanding of what to improve for version 2.

HyQ has 12 active DOF. Each leg has three hydraulically actuated joints: Hip Abduction/Adduction (HAA), Hip Flexion/Extension (HFE) and Knee Flexion/Extension (KFE) joint. Table II lists the main specifications of HyQ. Since its construction in 2010, HyQ demonstrated a wide repertoire of motions ranging from stair climbing [11], chimney climbing [35], omnidirectional trotting over rough terrain [12], trotting with step reflexes [36] to flying trotting [13] and jumping [14].

The last 5 years of experiments with HyQ allowed us to carefully assess the limitations of the machine. First of all, the mechanical structure is not robust to falls so we could never test the robot without its safety harness. This limitation made it impossible to test the robot in environments where a safety harness cannot be brought. Thus, experiments in realistic environments were difficult. Second, the 120 degrees range of motion of the HFE and KFE joint was too small, so the robot was not able to lower the torso to the ground to enter an *idle* mode between experiments/tasks. Additionally, the limited range of motion did not permit the robot to perform self-righting. As shown in Fig. 2 (left), the HFE and KFE joints are actuated by hydraulic cylinders that directly connect two leg segments through a hinge joint. A significantly larger range of motion is not feasible with such a simple mechanism, see Fig. 2 (right). Third, the torque profiles especially in the HFE joints sometimes limited the motion capabilities of the robot, e.g. during the chimney climbing motions as described in [35]. As can be seen in Fig. 2 the KFE (and HFE joints)

has a decreasing torque towards full leg extension and full leg retraction.

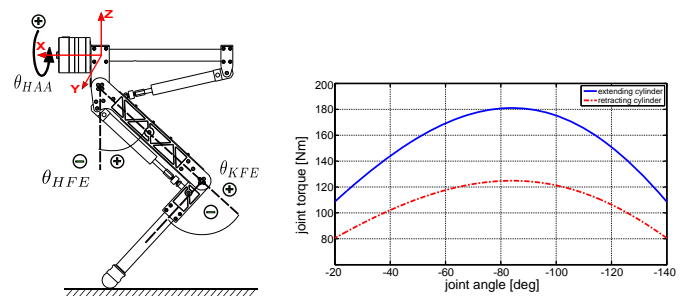


Fig. 2. Definition of HyQ leg angles and joint torque profiles. Left: Sketch of the left front (LF) leg with the definition of angles, joint names and leg base coordinate frame; Right: KFE maximum joint torque vs. cylinder position plot (at 20MPa).

These limitations will be addressed in the design of the new robot as follows: First, with a larger range of motion through modified kinematics (Section IV-B) and different actuator types and mechanisms (Section V-A). Second, with optimized cylinder and mechanism geometry (Section V-B), and third, with a more rugged mechanical structure (Section VI-A).

C. Required Motion Skills and Performance

The next step in the design process is to define specific motion skills and performance levels that match the requirement 2, 3 and 4 listed in Section III-A. We defined a list of 7 *characteristic motions* for quadrupeds. The selection is aimed to cover a wide range of different motions that represent normal and extreme cases that will lead to maximum values of joint range, torque, velocity and power. The first four motions include dynamic gaits like walking trot on rough/flat terrain, turning and push recovery under lateral perturbations. The other three motions include crawling, stair climbing and self-righting. The self-righting motion demonstrates both the self-righting capability and the ability to squat and lie down on the belly.

Note that none of the controllers of these motions is a contribution of this paper. All motions have been published before as indicated with the citations. We discuss the selection of these motions and their impact on the robot design in the discussion (Section VII).

The following list shows the 7 motions with the desired levels of target performance (e.g. speed for trotting and crawling).

- 1) RT: walking trot on rough terrain [12] (0.5m/s)
- 2) WT: walking trot on flat ground [12] (1.5m/s)
- 3) TR: walking trot with turning [12] (0.5m/s with 25deg/s turning)
- 4) PR: push recovery [12] (lateral perturbation of 500N for 1s)
- 5) CF: crawling on flat ground [37] (average speed 0.1m/s)
- 6) CS: stair climbing [11] (step height 0.12m and step depth 0.3m)
- 7) SR: self-righting (predefined motion as described in [15])

In Section IV, we will use these characteristic motions and performance levels to obtain simulation data that will help to size and select the joint actuators. See the supplementary material for a video showing all the 7 simulated motions.

IV. SIMULATION OF CHARACTERISTIC MOTIONS

In the previous section we defined the target application requirements of HyQ2Max and 7 characteristic motions that the new robot needs to be able to perform. This section describes how these 7 motions are simulated and presents the results that are later used for the selection and sizing of the joint actuators (Section V).

A. Rigid Body Dynamics Simulation and RobCoGen

Our simulation environment is composed of two software packages. The first, called *SL*, is a multi-process application that provides a low level joint controller, a customizable trajectory generator, and a rigid body dynamics simulator. The controller and the trajectory generator can seamlessly also run and control a real robot [38].

Second, the robot-specific software, namely the kinematics and dynamics engine, is implemented with *RobCoGen*. RobCoGen is a program that reads a simple robot description and *generates* an optimized C++ implementation of kinematics and dynamics [39], [40]. The code generated with RobCoGen is combined with SL, to obtain a fast rigid body dynamics simulation of the robot (for example, the SL simulator is programmed to use the forward dynamics implementation generated by RobCoGen). The dynamics engine uses spatial-vector algebra and state-of-the-art numerical algorithms [41].

We have validated the simulator with walking trot experiments performed on the HyQ robot. In our recent online technical report [42] we compared the joint torque/power plots of a 1m/s trot with the simulation results of the same motion. The simulation results approximate the experimental results sufficiently well, which allows us to use this simulation environment for the design of new robots.

B. Robot Model: Kinematics and Weight Distribution

To model the robot in simulation, we first have to define the kinematics and the weight distribution of the robot. This input can either be provided by an optimization of the robot morphology, by biological data of humans/animals or by the researchers' experience with earlier prototypes (see Section II-B). We will follow the last approach for HyQ2Max. See Section VII for a critical discussion on the assumptions and weaknesses of our design approach.

Kinematics: First of all, the robot kinematics will be based on the 12-DOF kinematics of HyQ, Fig. 3. Each leg has three DOF. Experiments with HyQ have shown that the X-configuration of the legs (front knees pointing to the hind knees, see page 55 of Semini's dissertation [43]) are suitable for a variety of behaviors, as described in Section III-B. Thus, we will use the same leg configuration for HyQ2Max.

HyQ's configuration of HAA and HFE joints, however, does not allow the robot to rotate the HFE joint sufficiently to allow

a self-righting motion of the robot. During self-righting, the feet need to be moved above the torso, which requires a large HFE range.

The simplest solution is to shift the leg's flexion/extension plane⁵ outward with respect to the HAA axis. Figure 3 (right) shows the updated kinematics for one leg.

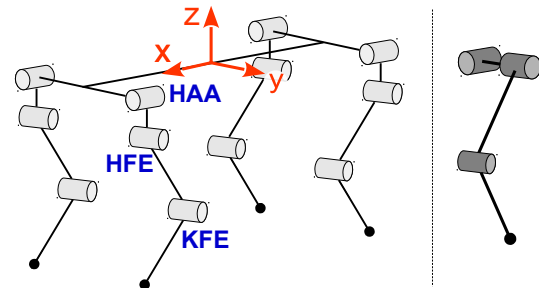


Fig. 3. Robot kinematics. Left: Kinematics of the 12-DOF HyQ robot showing the robot's base coordinate frame and the location of the three joints of the left front leg: hip abduction/adduction (HAA), hip flexion/extension (HFE) and knee flexion/extension (KFE); Right: Kinematics of a HyQ2Max leg.

The torso and link lengths for the initial model of the new robot were identical to HyQ.

Weight Distribution: Next, the weight distribution of the leg segments and torso have to be determined. Again, we use HyQ as base. As a conservative initial guess that accounts for more powerful actuators with a larger range of motion, we doubled the mass of each leg link of HyQ (see Table II). The mass of the torso is 29.6kg which is the required total mass of the robot (80kg) minus the weight of the four legs. All links are modelled as solid cylinders with homogeneously distributed mass (constant density) to obtain the rigid body model.

Last, to reduce design complexity we aim to use the same leg design for all the four legs.

C. Simulation Results of Characteristic Motions

This initial robot model was then implemented within the simulator through RobCoGen (Section IV-A). We performed several simulations to cover all the 7 characteristic motions. All simulations were run for 0kg payload (total robot mass 80kg) and for 40kg payload (robot mass 120kg). The payload was added to the torso mass and evenly distributed. As described in Section III-A, the 40kg extra weight represents a future extension with onboard power supply and payload. Therefore, we will only use the 40kg data logs for the design of the robot. See the supplementary material for a video showing all the 7 simulated motions.

The information contained in the resulting data logs is very rich, as it includes position, velocity and load profiles of all joints, ground reaction forces of all feet, body accelerations, overall mechanical power requirements etc. We will use position, torque and velocity (power) data to size joint actuators and valves (Section V).

We will first use the torque and position data to determine required joint range of motion and maximum torque profiles.

⁵The leg's flexion/extension plane is the plane that is normal to the HFE and KFE axes and intersects the center of the foot.

Figure 4 shows the joint torque vs. position plots for the three joints of the left front leg for all 7 characteristic motions with 40kg payload. The joint names and angle definitions are the same as in HyQ, see Fig. 2 (left) and [43].

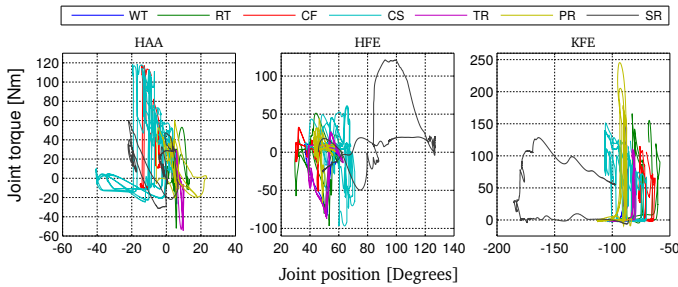


Fig. 4. Joint torque vs. joint position plots for the three leg joints of the left front leg, shown for the 7 characteristic motions with 40kg payload. See Section III-C for an explanation of the abbreviations.

V. MECHANISM OPTIMIZATION, ACTUATOR AND VALVE SIZING

This section will first analyze the torque profiles of the three joints to evaluate whether a linear or rotary actuator better fits the torque requirements. Subsequently, we will show how we optimized the cylinder size and four-bar linkage⁶ of the knee joint. Finally, the size of the valve is determined.

The motivation behind this optimization is to obtain torque profiles that approximate the required torques resulting from the simulations. Oversizing the hydraulic actuators has a negative impact on the required hydraulic flow of the machine and thus on its energy efficiency. The larger the actuator chamber the higher the required flow for the same velocity. In a system with fixed supply pressure, the sum of the flow rates Q of all joints i multiplied by the supply pressure p gives the instantaneous hydraulic power consumption P

$$P = \sum_{i=1}^{12} Q_i p \quad (1)$$

Other advantages of correctly sizing joint actuators are reduced actuator mass and smaller valve throttling losses that lead to a smaller onboard heat exchanger.

A. Linear vs. Rotary Actuators Comparison based on Torque Requirements

The two most common hydraulic actuator types are linear cylinders and rotary actuators. Rotary vane actuators are either single-vane (large range of motion typically around 270 degrees) or double-vane (double torque, but reduced range of motion of typically around 100 degrees). This actuator type produces a constant torque output independent from joint position, but usually has a lower torque-to-weight ratio. Hydraulic cylinders connected to a linkage are usually lighter,

⁶Four-bar linkages in combination with hydraulic cylinders are widely used in excavators. Some hydraulic robots use four-bar linkages, e.g. the humanoid robot CB developed by SARCOS Inc. [44]. Unfortunately, no information about the sizing of the linkage of this robot has been published.

but create a non-linear torque profile. Additionally, since the most commonly used cylinders have an asymmetric force output during extension and retraction, two motion-direction-dependent output torques need to be considered. These two properties of asymmetric cylinders mounted between two links are shown in Fig. 2 (right). We will show below how a cylinder connected to a four-bar linkage can be used to optimize the torque profiles to reduce unnecessarily high maximum torque during extension and retraction.

Since we aim to reuse the same leg design as much as possible on all the four legs, we have to merge the data of all the four legs into a single plot for each joint. The front leg pair has different torque requirements than the hind legs for all the motions except the self-righting. The same is true for the left and right leg pairs. For a correct merging of the data, the joint angle convention of the robot has to be carefully followed. Both HyQ and HyQ2Max have the same angle convention as defined in [43].

All **KFE joints** have a very asymmetric torque profile, requiring high torques for leg extension and low torques for leg retraction. This makes sense, as the knee joint mainly acts as load carrying joint during stance phases. The swing phases in which the leg is retracted require much lower torques due to the small inertia of the lower leg and foot (even at high speeds). The required range of motion is below 180 degrees. These requirements match well with the characteristics of a linear cylinder connected to a linkage mechanism, as we will explain in Section V-B.

The **HFE joint** and **HAA joint** on the other hand require from the actuators similar positive and negative torques. The range of motion required from the HFE joints goes well beyond 180 degrees. This matches well with a rotary single vane actuator. The HAA joints need to move less than 100 degrees, so a double vane rotary actuator is the preferred choice (double the torque output compared to the same size single vane actuator).

The next step is to select maximum torque outputs for these two rotary joints. Figure 5 shows the merged characteristic motion plots of the four legs separated into one plot for each of the three leg joints (see also Fig. 4).

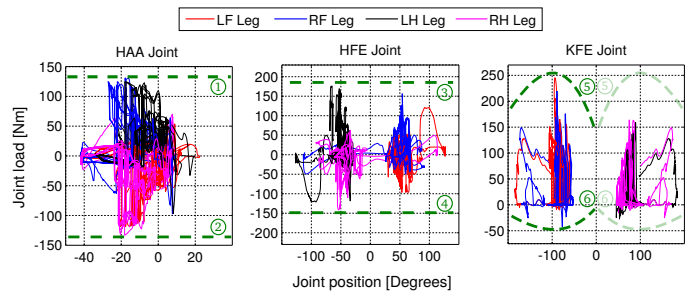


Fig. 5. Joint load vs. position plots of the 7 motions for a robot model with 120kg mass (40kg payload). The plots of the four legs are merged according to the robot's angle conventions [43]. The HAA/HFE joints are implemented with rotary actuators and the KFE joint is actuated by a linear one. The green dashed lines indicate the torque limits to be used to size the actuators.

We added green dashed lines to the plots to indicate the desired limits that enclose the negative and positive joint torque

requirements. The rotary vane actuators have positive/negative symmetric torque limits that are constant throughout the entire joint range. The limits are thus represented by straight lines. The cylinder and four-bar linkage of the KFE joint creates a non-linear profile and can be approximated with a polynomial as explained in detail in the next section.

We can now select the sizes of the two rotary actuators based on these plots and the availability on the market. As not many manufacturers sell small-size rotary vane actuators, the selection is limited. For the HAA joint we selected the same hydraulic rotary double vane actuator as in the HAA joint of HyQ with 120Nm maximum torque at 20MPa. This is slightly below the peaks of the simulated maximum torques, but preferred since the next bigger size is too large. With 1kg weight the actuator is light and compact.

For the HFE joint we selected a single vane actuator with 245Nm maximum torque at 20MPa. This is not optimal since it exceeds the required torque by more than 50Nm. However, the actuator that is one size smaller would not provide sufficient torque. As mentioned in Section VIII, in the future we will replace the current rotary actuators with custom-made actuators to better match the required maximum torque.

B. Optimization of Hydraulic Actuator Sizes and Four-bar Linkage Mechanism

In comparison to a simple hinge, the four-bar linkage mechanism can provide a more constant output torque for the same joint range of motion. The many links present in this mechanism can be seen as degrees of freedom that can be adjusted to better fit the output torques to a specific target curve. In this section we describe the optimization-based method we use to dimension such links and the respective pivot points in order to obtain a desired KFE torque profile.

As target curve for the KFE torque profile we considered the dashed line number 5 shown in Fig. 5. This line is mathematically approximated by a polynomial function $T_{target}(\theta)$, where θ is the KFE joint angle.

Figure 6 illustrates the four-bar linkage mechanism that connects the KFE cylinder to the lower leg. The whole mechanism is parametrized according to the pivot positions $\vec{A} = (A_x, A_y)$ and $\vec{C} = (C_x, C_y)$ described in the reference frame located at point H , to relative distances ($l_{ra} = \vec{R}A$, $l_{rb} = \vec{R}B$ and $l_{kb} = \vec{K}B$) and to the angle $fk b$ between the points F , K and B .

With this parametrization we derive the Jacobian $J(\theta)$ that describes the relationship between cylinder force F_{cyl} and joint torque $T(\theta)$ as:

$$T(\theta) = J^T(\theta) \cdot F_{cyl} \quad (2)$$

The goal of the optimization is to find the parameter values that minimize the error between the output torque $T(\theta)$ and the desired output torque $T_{target}(\theta)$, given geometrical constraints defined by the space available to allocate the mechanism inside the upper leg shell. Considering also the maximum cylinder

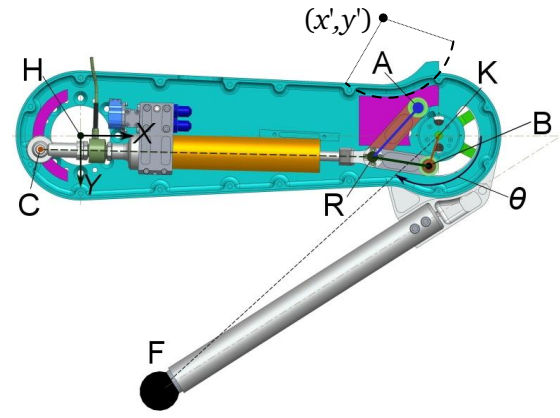


Fig. 6. Mechanical design and parametrization of the KFE cylinder mounting and four-bar linkage mechanism for the left-front and right-hind legs (these two legs have an identical design). The pink regions on the left and right are the constrained areas to position the pivot points \vec{C} and \vec{A} , respectively.

force F_{max} as a decision variable, the cost function to be minimized is defined as:

$$\sum_{\theta=0.35}^{2.93} (J^T(\theta) \cdot F_{max} - T_{target}(\theta))^2 \quad (3)$$

subject to the following inequality constraints:

$$0.03 \leq \sqrt{(A_x - K_x)^2 + (A_y - K_y)^2} \quad (4)$$

$$0.037 \leq \sqrt{C_x^2 + C_y^2} \leq 0.048 \quad (5)$$

$$\sqrt{(A_x - x')^2 + (A_y + y')^2} \geq 0.062 \quad (6)$$

$$\sqrt{(A_x - x')^2 + (A_y - y')^2} \geq 0.064 + l_{ra} \quad (7)$$

$$\frac{0.013}{0.0280} A_x - A_y - 0.053 \leq 0 \quad (8)$$

where the inequality constraints limit the positions \vec{A} and \vec{C} to be inside the pink regions illustrated in Fig. 6. The cost function is minimized for $\theta \in [0.35, 2.93]$, which is the joint range of interest. To also respect the space available inside the shell, the optimization variables are constrained to the following intervals: $A_x \in [0.028, 0.036]$, $A_y \in [-0.05, 0.01]$, $C_x \in [-0.05, -0.013]$, $C_y \in [-0.046, 0.046]$, $l_{ra} \in [0.025, 0.07]$, $l_{rb} \in [0.025, 0.07]$, $l_{kb} \in [0.032, 0.034]$, $F_{max} \in [1, 6] \cdot 10^3$ and $fk b \in [0.68, 0.70]$. All distances are described in meters, the cylinder area in m^2 and angles in radians.

The output obtained from the optimizer is: $A_x = 0.0339$, $A_y = -0.0281$, $C_x = -0.0404$, $C_y = 0.0140$, $l_{ra} = 0.0674$, $l_{rb} = 0.0566$, $l_{kb} = 0.0323$, $F_{max} = 5.66 \cdot 10^3$ and $fk b = 0.687$.

This solution defines a mechanism that is able to realize the desired KFE output torque profile with a maximum error of 5Nm.

Next, we will size the hydraulic actuators using another optimization algorithm where the dynamic requirements (joint load and velocity) from the characteristic motions are considered. All the characteristic motions' data is concatenated in vectors that, through the four-bar linkage kinematics, are post-processed to obtain actuator efforts and velocities. Taking

into account the hydraulics relationships that associate chamber pressures/flows with actuator parameters, the volumetric displacement of the HAA and HFE joint actuators ($h_{aa_{vd}}$ and $h_{fe_{vd}}$, respectively) and the cylinder areas for the KFE joints ($k_{fe_{Aa}}$ and $k_{fe_{Ab}}$) are obtained through a cost function that minimizes the hydraulic power for a fixed supply pressure $P_s = 20MPa$. Such optimization problem is defined as:

$$\sum_{j=1}^{12} \sum_{k=1}^n (P_s \cdot Q_{jk})^T W_{k,k} (P_s \cdot Q_{jk}) \quad (9)$$

where Q_{jk} stands for the k -th flow demand of the joint j and $W \in \mathbb{R}^{i \times i}$ is the diagonal weighting matrix that is used to penalize each characteristic motion according to the motion relevance. The cost function is minimized for $h_{aa_{vd}} \in [6.87 \cdot 10^{-7}, 6.87 \cdot 10^{-5}]$, $h_{fe_{vd}} \in [1.43 \cdot 10^{-6}, 1.43 \cdot 10^{-4}]$, $k_{fe_{Aa}} \in [3.14 \cdot 10^{-5}, 3.14 \cdot 10^{-3}]$ and $k_{fe_{Ab}} \in [2.00 \cdot 10^{-5}, 2.00 \cdot 10^{-3}]$. Moreover, to avoid a solution set that leads to the need of negative chamber pressures, inequality constraints were introduced so that the minimum pressure in any chamber must be greater than 1MPa.

The output obtained from the optimizer is: $h_{aa_{vd}} = 8.91e-6 m^2$, $h_{fe_{vd}} = 1.007e-5 m^2$, $k_{fe_{Aa}} = 3.365e-4 m^2$ (equivalent to a bore diameter of 0.0207 m) and $k_{fe_{Ab}} = 8.3147e-5 m^2$ (corresponding to a rod diameter of 0.01797 m).

For this version of HyQ2Max we selected only commercially available actuators. See Section V-A for the selected actuators for HAA and HFE joints. For the KFE we selected a Hoerbiger LB6-2012 cylinder with a bore and rod diameter of 0.020m and 0.012m, respectively. While the bore size matches well the optimized value, the rod diameter is too small, which leads to an oversized piston annulus area. An optimized cylinder size will lead to smaller hydraulic oil flow and thus reduced energy consumption.

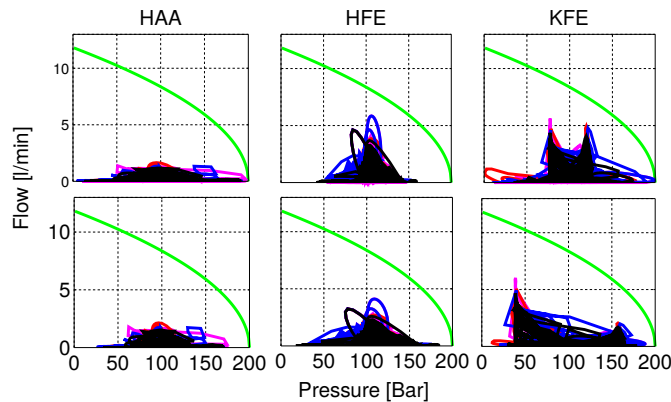


Fig. 7. Flow vs. pressure plots of the characteristic motions for all the three joints comparing the selected commercially available actuators (top row) with the optimized ones (bottom row). The green line indicates the maximum flow rate of the Moog E024 valve used on HyQ2Max (7.0l/min at 7MPa pressure drop).

Last, we will use again the torque and velocity signals to plot the flow vs. pressure plots to analyze the valve size. Figure 7 shows the flow vs. pressure plots of the characteristic motions for all the three joints comparing the selected commercially available actuators (top row) with the optimized

ones (bottom row). The green line indicates the maximum flow rate of the Moog E024 valve used on HyQ2Max (7.0l/min at 7MPa pressure drop). The supply pressure is considered to be fixed to 20MPa. The plots show that all the flow requirements are below the valve limit, and that the pressure demand of the optimized actuators stays further away from the pressure limits compared to non-optimized ones. The plots also show that a valve with a smaller rated flow would have still met the requirements. This would increase the flow control resolution, at the expense of a lower control bandwidth. A more detailed study is required to optimize this parameter.

VI. DESIGN OF HYQ2MAX AND FIRST EXPERIMENTAL RESULTS

This section will present the final design of the HyQ2Max robot, list the system specifications and show the results of initial experiments.

A. HyQ2Max Design and Specifications

The robot was designed according to the requirements listed in Section III-A. Figure 8 shows the CAD model of the robot with the right front upper leg opened to show the cylinder and the optimized four-bar linkage. This version of the robot weighs 80kg without an onboard power supply. However, the joint actuators are sized for a future upgrade into a power-autonomous version (with a total robot weight of 120kg including payload), see Section III and V.

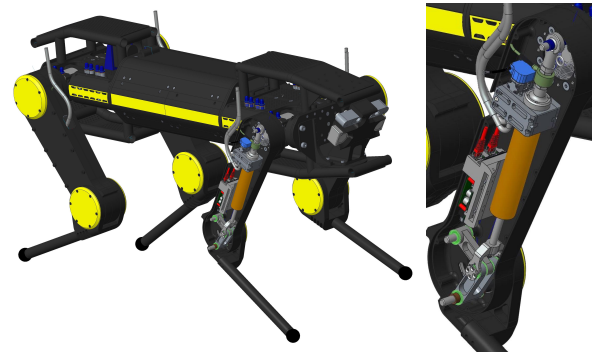


Fig. 8. CAD images of HyQ2Max. *Left*: The right front upper leg is opened to show the hydraulic cylinder and four-bar linkage of the knee joint that were optimized in Section V. *Right*: Close-up view of the upper leg showing hydraulic cylinder, valve, manifold, electronics and four-bar linkage.

The majority of the structural parts are built in aerospace-grade aluminium alloy (type 7075). Rugged leg shells (upper leg) and tubular structures (torso) protect delicate electronics, sensors and actuators. The central section of the torso that contains the computers, electric power/safety management and hydraulic system is protected by Kevlar reinforced fibre composite covers.

Figure 9 shows the front, side and section views of the robot CAD, including the overall dimensions and the major design details. The torso and leg structures are built so that the robot does not get damaged during falls and subsequent self-righting motions when rolling from an upside-down posture onto its side and back to its feet.

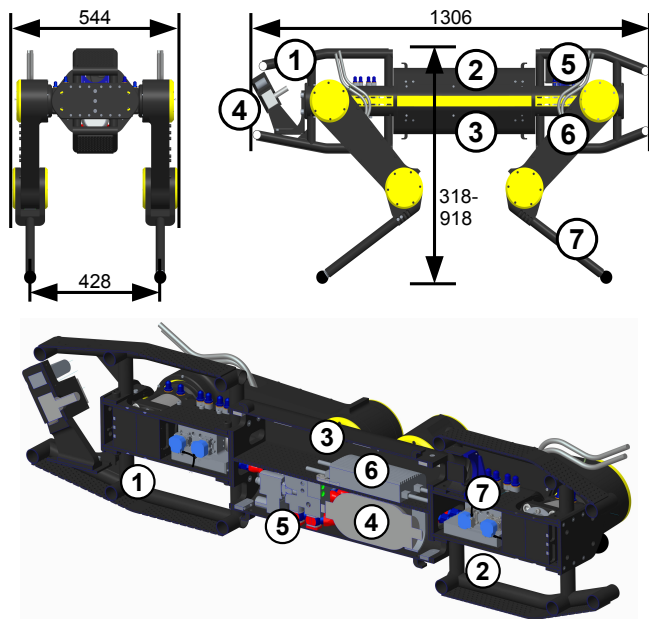


Fig. 9. Dimensions and design details of HyQ2Max. *Top*: Frontal and lateral view of HyQ2Max CAD showing the overall dimensions (in mm) of the robot. The numbers describe the main parts and details of the robot: (1) protective cage with aluminium bars; (2) upper half of central torso section with electronics; (3) lower half of central torso section with hydraulics; (4) Perception system; (5) hydraulic hoses and electric wires from torso to upper leg; (6) upper leg shells; (7) lower leg tube and rubber foot. *Bottom*: Section view through the sagittal plane of the robot CAD model with numbered details: (1) front section of torso; (2) hind section of torso; (3) central section of torso; (4) hydraulic accumulator; (5) hydraulic manifold with pressure relief valve and vent valve for safety; (6) onboard computer for locomotion control; (7) hydraulic manifold for each leg connecting 2 valves and the HAA motor.

The hydraulic system of the robot includes highly integrated hydraulic leg manifolds that are produced with additive manufacturing of AlSiMg aluminium alloy (direct metal laser sintering). The interested reader is referred to [45] for more details on the manifolds and the hydraulic system of the robot.

Each joint features high-resolution absolute encoders (IC-Haus/Balluff 19-bit) and custom torque sensors or load cells (Futek LCM 325). The same servovalves (MOOG E024) as in HyQ are used for high-performance joint torque control [46]. Table III gives an overview of the specifications of the robot.

B. Experimental Results

HyQ2Max has recently been built and we tested its capabilities during trotting and self-righting. The robot weighed 80kg during the experiments since the power was offboard and no payload was added. Figure 10 shows the torque profiles of the four legs during a self-righting motion and the torque, ground reaction force, position and power plots during a walking trot. The supplementary material contains a video showing this trotting motion and the self-righting experiment performed on HyQ2Max. The interested reader is referred to [15] for more information on the self-righting sequence.

VII. DISCUSSION

This section discusses some of the weaknesses related to the presented approach to select and size actuators.

TABLE III
SYSTEM OVERVIEW OF THE HYQ2MAX ROBOT

dimensions	1.306m x 0.544m x 0.918m (LxWxH)
distance left/right HAA	0.194m from axis to axis
distance front/hind HFE	0.887m from axis to axis
link lengths & weights	hip (HAA-HFE): 0.10m, 3.54kg upper leg (HFE-KFE): 0.36m, 4.95kg lower leg (KFE-foot): 0.38m, 1.40kg
maximum leg length	0.724m (from HFE axis to center of foot)
weight	80kg (offboard power)
active DOF	12
HAA actuators	double-vane rotary hydraulic actuators
HFE actuators	single-vane rotary hydraulic actuators
KFE actuators	asymm. hyd. cylinders & four-bar linkage
joint motion range	80° (HAA), 270° (HFE), 165° (KFE)
max. torque [HAA]	120Nm (constant torque at 20MPa)
max. torque [HFE]	245Nm (constant torque at 20MPa)
max. torque [KFE]	250Nm (peak torque at 20MPa)
position sensors	absolute position 262,144cpr in all joints
torque/load sensors	torque (HAA, HFE), load cell (KFE)
onboard computer	Pentium i5 with real-time Linux
controller rate	1kHz torque & position control (EtherCAT)

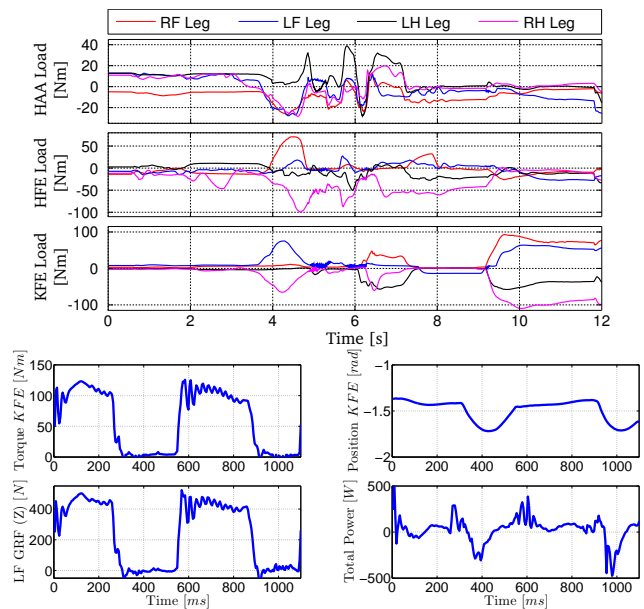


Fig. 10. Experimental results of self righting and a walking trot experiment with HyQ2Max. *Top*: Self righting: Joint torque vs. time plots for the four legs divided into the three leg joints. *Bottom*: Walking trot: The left plot shows the knee torque of the left front leg and the same leg's ground reaction forces. The right plot shows the position of the left front knee joint and the total mechanical power of all the 12 joints.

One of the weaknesses is that the selection of the characteristic motions and their controllers have an influence on the obtained size of the actuators. Our selection of the 7 motions is heavily influenced by the availability of already implemented and tested controllers. In our case, the control parameters were manually tuned by an expert, instead of using optimization. Furthermore, we selected a robot morphology based on the previous version of the robot, instead of opening it up for optimization.

We took this path, because the search space of the parameters that define robot morphology, kinematic structure and actuators is so large that an optimization is very difficult. Furthermore, the various locomotion controllers and

motion planners are part of the search space, e.g. which gait (walk/trot/gallop) and what gait parameters (step length and frequency) are most optimal for a given situation. As briefly mentioned in Section II-B as category (d), some researchers use optimization of robot morphology and joint requirements. Examples can mainly be found in the Computer Graphics communities where the morphology, actuator location and control of several robot model are optimized with evolutionary algorithms. Geijtenbeek et al. [30] simulated bipedal creatures with biomechanical muscle models. The authors claim that the synthesized controllers find different gaits based on the target speed, can cope with uneven terrain and external perturbations, and can steer to target directions. Digumarti et al. [31] used concurrent optimization to improve the kinematics and controllers of the electric quadruped robot StarLETH to be used as guidelines for future versions of the robot. The approach is based on a locomotion optimization framework [47] that automatically finds parameters for agile gaits. In the study of Digumarti et al. the robot morphology was optimized for faster running. The actuators on the other hand were not part of the optimization.

The state of the art in legged robot design is still far from converging to an established and widely accepted best practice. We think that a systematic design method has to include input from various fields such as machine design, locomotion control and computer graphics. We believe that the approach described in this paper is an important puzzle piece that can be nicely combined with other state of the art methods.

VIII. CONCLUSIONS

This paper presented the design of the new hydraulic quadruped robot HyQ2Max. As evolution of the torque-controlled HyQ robot, the new version needs to be more rugged, more powerful and extend HyQ's locomotion skills with self-righting capability. To obtain suitable joint requirements, we simulated 7 characteristic motions ranging from trotting on rough terrain, stair climbing, to push recovery. Subsequently, we merged the simulation results and used the joint angle and torque profiles to evaluate whether a rotary or linear hydraulic actuator is more suitable for each of the three leg joints. Rotary vane actuators are better for the HAA and HFE joints due to the required range of motion and shape of torque profiles. For the KFE joint we selected a linear actuator with four-bar linkage, since the knee joints need to produce large torques in one direction (leg extension) and much smaller torques in the other (leg retraction). We described in detail how we optimized the cylinder size and linkage parameters.

As one of the three contributions of this paper, we explained how to correctly size the cylinder's bore and rod diameter to best fit the requirements and thus reduce the joint's hydraulic flow rate and power demand. After the presentation of the overall robot design and specifications, we showed the results of successful self-righting and trotting experiments. The paper is rounded up with a discussion on the weaknesses of the presented approach.

In the future we will install a multi-pump hydraulic power supply system into a larger-sized torso to make HyQ2Max

power-autonomous. In parallel, we intend to replace our standard hydraulic actuators with customized components.

We will also try to extend our actuator selection approach to variable supply pressures and merge it with evolutionary algorithms that help to optimize robot morphology, kinematics, gaits, actuators and power supply systems.

MULTIMEDIA EXTENSION

The supplementary material contains a video showing the simulation of the 7 characteristic motions and experimental results of HyQ2Max demonstrating self-righting and trotting.

ACKNOWLEDGMENT

This research was funded by the Fondazione Istituto Italiano di Tecnologia. The authors would like to thank also the other members of the Dynamic Legged Systems Lab that contributed to the success of this project: A. Posatskiy, B. Rehman, C. Mastalli, M. Camurri, R. Orsolino and former members (I. Havoutis, S. Bazeille, H. Khan). The HyQ2Max robot was designed by J. Goldsmith. A special thank goes to G. Rey and M. Baker of MOOG Inc. for the fruitful discussions on various topics covered in this paper.

REFERENCES

- [1] J. Cortell and A. Ruina, "Actuator design for a high-performance legged biped robot," in *Dynamic Walking Conference*, 2014.
- [2] S.-H. Hyon, T. Yoneda, and D. Suewaka, "Lightweight hydraulic leg to explore agile legged locomotion," in *IEEE/RSJ International Conference on Intelligent Robots and Systems (IROS)*, Nov 2013, pp. 4655–4660.
- [3] S. Seok, A. Wang, D. Otten, and S. Kim, "Actuator design for high force proprioceptive control in fast legged locomotion," in *IEEE/RSJ International Conference on Intelligent Robots and Systems (IROS)*, Oct 2012, pp. 1970–1975.
- [4] C. Semini, N. G. Tsagarakis, E. Guglielmino, M. Focchi, F. Cannella, and D. G. Caldwell, "Design of HyQ – a hydraulically and electrically actuated quadruped robot," *Journal of Systems and Control Engineering*, vol. 225, pp. 831–849, 2011.
- [5] H. Khan, C. Semini, V. Barasuol, and D. G. Caldwell, "Actuator sizing for highly-dynamic quadruped robots based on squat jumps and running trots," in *International Conference on Climbing and Walking Robots (CLAWAR)*, 2013.
- [6] P. Chatzakos and E. Papadopoulos, "The influence of dc electric drives on sizing quadruped robots," in *IEEE International Conference on Robotics and Automation (ICRA)*, May 2008, pp. 793–798.
- [7] B. T. Krupp and J. E. Pratt, "A power autonomous monopedal robot," in *SPIE 6201*, 2006.
- [8] E. Garcia, J. C. Arevalo, G. Muñoz, and P. Gonzalez-de Santos, "On the biomimetic design of agile-robot legs," *Sensors*, vol. 11, no. 12, pp. 11 305–11 334, 2011.
- [9] Y. Ito, S. Nozawa, J. Urata, T. Nakaoka, K. Kobayashi, Y. Nakanishi, K. Okada, and M. Inaba, "Development and verification of life-size humanoid with high-output actuation system," in *IEEE International Conference on Robotics and Automation (ICRA)*, 2014, pp. 3433–3438.
- [10] H. Khan, S. Kitano, M. Frigerio, M. Camurri, V. Barasuol, R. Featherstone, D. G. Caldwell, and C. Semini, "Development of the lightweight hydraulic quadruped robot - MiniHyQ," in *IEEE International Conference on Technologies for Practical Robot Applications (TEPRA)*, 2015.
- [11] A. Winkler, C. Mastalli, I. Havoutis, M. Focchi, D. G. Caldwell, and C. Semini, "Planning and execution of dynamic whole-body locomotion for a hydraulic quadruped on challenging terrain," in *IEEE International Conference on Robotics and Automation (ICRA)*, May 2015.
- [12] V. Barasuol, J. Buchli, C. Semini, M. Frigerio, E. R. D. Pieri, and D. G. Caldwell, "A reactive controller framework for quadrupedal locomotion on challenging terrain," in *IEEE International Conference on Robotics and Automation (ICRA)*, 2013.
- [13] C. Semini, V. Barasuol, T. Boaventura, M. Frigerio, M. Focchi, D. G. Caldwell, and J. Buchli, "Towards versatile legged robots through active impedance control," *The International Journal of Robotics Research (IJRR)*, vol. 34, no. 7, pp. 1003–1020, 2015.
- [14] C. Semini, H. Khan, M. Frigerio, T. Boaventura-Cunha, M. Focchi, J. Buchli, and D. G. Caldwell, "Design and scaling of versatile quadruped robots," in *International Conference on Climbing and Walking Robots (CLAWAR)*, 2012, pp. 273–280.

- [15] C. Semini, J. Goldsmith, B. U. Rehman, M. Frigerio, V. Barasuol, M. Focchi, and D. G. Caldwell, "Design overview of the hydraulic quadruped robots HyQ2Max and HyQ2Centaur," in *The Fourteenth Scandinavian International Conference on Fluid Power (SICFP)*, 2015.
- [16] R. Liston and R. Mosher, "A versatile walking truck," in *Transportation Engineering Conference*, 1968.
- [17] M. Raibert, *Legged Robots That Balance*. The MIT Press, 1986.
- [18] R. Hodoshima, T. Doi, Y. Fukuda, S. Hirose, T. Okamoto, and J. Mori, "Development of quadruped walking robot titan xi for steep slopes - slope map generation and map information application," *Journal of Robotics and Mechatronics*, vol. 19, pp. 13–26, 2007.
- [19] M. Raibert, K. Blankespoor, G. Nelson, R. Playter, and the Big-Dog Team, "Bigdog, the rough-terrain quadruped robot," in *World Congress of the International Federation of Automatic Control (IFAC)*, 2008.
- [20] X. Rong, Y. Li, J. Ruan, and B. Li, "Design and simulation for a hydraulic actuated quadruped robot," *Journal of Mechanical Science and Technology*, vol. 26, no. 4, pp. 1171–1177, 2012.
- [21] F. Gao, C. Qi, Q. Sun, X. Chen, and X. Tian, "A quadruped robot with parallel mechanism legs," in *IEEE International Conference on Robotics and Automation (ICRA)*, 2014.
- [22] J. Gao, X. Duan, Q. Huang, H. Liu, Z. Xu, Y. Liu, X. Li, and W. Sun, "The research of hydraulic quadruped bionic robot design," in *ICME International Conference on Complex Medical Engineering (CME)*, 2013, pp. 620–625.
- [23] C. RunBin, C. YangZheng, L. Lin, W. Jian, and M. H. Xu, "Inverse kinematics of a new quadruped robot control method," *International Journal Advanced Robotic Systems*, vol. 10, no. 46, 2013.
- [24] J. T. Kim, J. S. Cho, B.-Y. Park, S. Park, and Y. Lee, "Experimental investigation on the design of leg for a hydraulic actuated quadruped robot," in *44th International Symposium on Robotics (ISR)*, 2013.
- [25] K. Kawabata, T. Nishi, Y. Torii Kitaur, K. Kanematsu, and S.-H. Hyon, "Development of hydraulic quadruped walking robot "RL-A1"," *The Robotics and Mechatronics Conference (ROBOMECH)*, 2014.
- [26] A. De, G. Lynch, A. Johnson, and D. Koditschek, "Motor sizing for legged robots using dynamic task specification," in *IEEE International Conference on Technologies for Practical Robot Applications (TEPRA)*, 2011, pp. 64–69.
- [27] K. Kaneko, S. Kajita, F. Kanehiro, K. Yokoi, K. Fujiwara, H. Hirukawa, T. Kawasaki, M. Hirata, and T. Isozumi, "Design of advanced leg module for humanoid robotics project of meti," in *IEEE International Conference on Robotics and Automation (ICRA)*, 2002, pp. 38–45 vol.1.
- [28] H. Dallali, M. Mosadeghzad, G. Medrano-Cerda, V.-G. Loc, N. Tsagarakis, D. G. Caldwell, and M. Gesino, "Designing a high performance humanoid robot based on dynamic simulation," in *European Modelling Symposium (EMS)*, Nov 2013, pp. 359–364.
- [29] X. Rong, Y. Li, J. Meng, and B. Li, "Design for several hydraulic parameters of a quadruped robot," *Applied Mathematics & Information Sciences*, 2014.
- [30] T. Geijtenbeek, M. van de Panne, and A. F. van der Stappen, "Flexible muscle-based locomotion for bipedal creatures," *ACM Transactions on Graphics*, vol. 32, no. 6, 2013.
- [31] K. M. Digumarti, C. Gehring, S. Coros, J. Hwangbo, and R. Siegwart, "Concurrent optimization of mechanical design and locomotion control of a legged robot," in *International conference on climbing and walking robots (CLAWAR)*, 2014.
- [32] S. Lohmeier, T. Buschmann, M. Schwienbacher, H. Ulbrich, and F. Pfeiffer, "Leg design for a humanoid walking robot," in *6th IEEE-RAS International Conference on Humanoid Robots*, Dec 2006, pp. 536–541.
- [33] H. Khan, R. Featherstone, D. G. Caldwell, and C. Semini, "Bio-inspired knee joint mechanism for a hydraulic quadruped robot," in *International Conference on Automation, Robotics and Applications (ICARA)*, 2015.
- [34] M. Hutter, C. Gehring, M. Bloesch, M. Hoepflinger, C. D. Remy, and R. Siegwart, "StarLETH: a compliant quadrupedal robot for fast, efficient, and versatile locomotion," in *International Conference on Climbing and Walking Robots (CLAWAR)*, 2012.
- [35] M. Focchi, A. del Prete, I. Havoutis, R. Featherstone, D. G. Caldwell, and C. Semini, "High-slope terrain locomotion for torque-controlled quadruped robots," *Autonomous Robots*, pp. 1–14, 2016.
- [36] M. Focchi, V. Barasuol, I. Havoutis, J. Buchli, C. Semini, and D. G. Caldwell, "Local reflex generation for obstacle negotiation in quadrupedal locomotion," in *International Conference on Climbing and Walking Robots (CLAWAR)*, 2013.
- [37] A. Winkler, I. Havoutis, S. Bazeille, J. Ortiz, M. Focchi, D. G. Caldwell, and C. Semini, "Path planning with force-based foothold adaptation and virtual model control for torque controlled quadruped robots," in *IEEE International Conference on Robotics and Automation (ICRA)*, 2014.
- [38] S. Schaal, "The SL simulation and real-time control software package," CLMC lab, University of Southern California, Tech. Rep., 2009.
- [39] M. Frigerio, J. Buchli, and D. G. Caldwell, "Code generation of algebraic quantities for robot controllers," in *IEEE/RSJ International Conference on Intelligent Robots and Systems (IROS)*, 2012.
- [40] M. Frigerio, J. Buchli, D. G. Caldwell, and C. Semini, "RobCoGen: a code generator for efficient kinematics and dynamics of articulated robots, based on Domain Specific Languages," *Journal of Software Engineering for Robotics (JOSER)*, vol. 7, no. 1, pp. 36–54, 2016.
- [41] R. Featherstone, *Rigid Body Dynamics Algorithms*. Springer, 2008.
- [42] M. Frigerio, V. Barasuol, M. Focchi, and C. Semini, "Validation of computer simulations of the HyQ robot," Department of Advanced Robotics, Istituto Italiano di Tecnologia, Tech. Rep., 2016, (uploaded to arXiv: <http://arxiv.org/abs/1604.06818>).
- [43] C. Semini, "HyQ – design and development of a hydraulically actuated quadruped robot," Ph.D. dissertation, Istituto Italiano di Tecnologia (IIT) and University of Genova, 2010.
- [44] G. Cheng, S. Hyon, J. Morimoto, A. Ude, J. G. Hale, G. Colvin, W. Scroggin, and S. C. Jacobsen, "CB: A humanoid research platform for exploring neuroscience," *Advanced Robotics*, vol. 21, no. 10, pp. 1097–1114, 2007.
- [45] C. Semini, J. Goldsmith, D. Manfredi, F. Cagnano, E. Ambrosio, J. Pakkanen, and D. Caldwell, "Additive manufacturing for agile legged robots with hydraulic actuation," in *International Conference on Advanced Robotics (ICAR)*, 2015, pp. 123–129.
- [46] T. Boaventura, C. Semini, J. Buchli, M. Frigerio, M. Focchi, and D. G. Caldwell, "Dynamic torque control of a hydraulic quadruped robot," in *IEEE International Conference in Robotics and Automation (ICRA)*, 2012, pp. 1889–1894.
- [47] C. Gehring, S. Coros, M. Hutter, M. Bloesch, P. Fankhauser, M. Hoepflinger, and R. Siegwart, "Towards automatic discovery of agile gaits for quadrupedal robots," in *IEEE International Conference on Robotics and Automation (ICRA)*, May 2014, pp. 4243–4248.



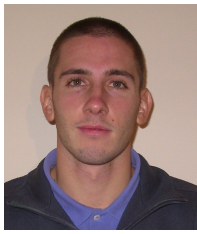
Claudio Semini received an M.Sc. degree in electrical engineering and information technology from ETH Zurich (2005). He is currently the Head of IIT's Dynamic Legged Systems (DLS) lab. From 2004 to 2006, he visited the Hirose Laboratory at Tokyo Tech, and the Toshiba R&D Center, Japan. During his doctorate (2007-2010) at the IIT, he developed the quadruped robot HyQ. After a postdoc with the same department, in 2012, he became the head of the DLS lab. His research interests include the construction and control of highly dynamic and versatile legged robots in real-world environments.



Victor Barasuol is a senior postdoctoral researcher at the Advanced Robotics Dept. at IIT. He holds a Diploma in Electrical Engineering from Universidade do Estado de Santa Catarina - UDESC (2006). He obtained an M.Sc. degree in Electrical Engineering (2008) and a doctorate degree in Automation and Systems Engineering (2013) from Universidade Federal de Santa Catarina - UFSC. He is currently a Post-Doc researcher at IIT's Dynamic Legged Systems lab and his research focus lies on the motion generation and control for quadruped robots with emphasis in dynamic and reactive locomotion.



Jake Goldsmith received BSc in Product Design from the University of Brunel, London in 2004. During which time he specialized in mechatronics. In 2004 he was employed by the Shadow Robot Company in London as a Robotics Engineer, working with their dexterous manipulator. In 2011 he moved to Italy to work at the IIT as a Design Engineer for the DLS lab, developing the new version of the HyQ, HyQ2Max. Jake is currently working as a Mechanical Engineer at Boston Dynamics.



Marco Frigerio received his B.Sc. and M.Sc. degrees in computer science from the University of Milano Bicocca, respectively in 2006 and 2008, and the Ph.D. degree in Robotics from the Istituto Italiano di Tecnologia (IIT) in 2013. He is currently a Post-Doc researcher at the Dynamic Legged Systems lab of IIT, where he is involved in the development of hydraulic legged robots. His research interests include software for robotics, software architectures, kinematics and dynamics of mechanisms.



Michele Focchi received the M.Sc. degree in Control System Engineering from Politecnico di Milano in 2007. He is currently a Post-Doc researcher in IIT's Dynamic Legged Systems (DLS) lab. In 2007 he worked on dynamic modelling of hydraulic turbines at the Federal University of Santa Catarina, Brazil. Until 2009 he worked in the R&D department of Indesit. In 2010 he started a PhD at IIT's DLS lab on the development of low-level controllers for locomotion purposes. Currently his research interests range from dynamic locomotion, model identifica-

tion to whole body control and planning.



Yifu Gao received the B. Sc. and M. Sc. degrees in mechanical engineering from Harbin Institute of Technology, Harbin, China, in 2008 and 2010. He is a Ph. D candidate in Dynamic Legged System Laboratory, Department of Advanced Robotics, Italian Institute of Technology, Genova, Italy since 2015. His research interests include mechanism and structure of legged robots, robotic arm and gripper, hydraulic actuator and circuit design and development for quadruped robot.



Darwin G. Caldwell received the B.S. and Ph.D. degrees in robotics from University of Hull, Hull, U.K., in 1986 and 1990, respectively, and the M.Sc. degree in management from University of Salford, Salford, U.K., in 1996. He is the Director of Robotics with Italian Institute of Technology, Genova, Italy. He is a Visiting/Honorary/Emeritus Professor with University of Sheffield, the University of Manchester, and University of Wales, Bangor. His research interests include innovative actuators and sensors, haptic feedback, force augmentation exoskeletons, dexterous manipulators, humanoid robotics, biomimetic systems, rehabilitation robotics, and telepresence and teleoperation procedures.